



Antimicrobial action of Tamarind-Synthesized Selenium Nanoparticles against *Helicobacter pylori*

Walaa F. Abdelqawi¹, Sabha M. El-Sabbagh², Soha A. El-Hady¹ and Ahmed A. Tayel³

¹Nasser Institute Hospital for Research and Treatment, Cairo, Egypt.

²Department of Botany and Microbiology, Faculty of Science, Menoufia University, Menoufia 32511, Egypt.

³Department of Fish Processing and Biotechnology, Faculty of Aquatic and Fisheries Sciences, Kafrelsheikh University, Kafrelsheikh 33516, Egypt

Received: 10 Nov. 2023

Accepted: 25 Dec. 2023

Published: 10 Jan. 2024

ABSTRACT

Helicobacter pylori is a significant bacterium with implications for gastrointestinal health, ranging from benign conditions like gastritis to more serious outcomes such as stomach cancer. The nanomaterials' applications is regarded as potential remedies for microbial infections. The extract of *Tamarindus indica* (Tamarind) fruits was employed for biosynthesis of selenium nanoparticles (SeNPs). The fruit extract was used as a good capping and stabilizing agent and allowed the formation of stable nanoparticles. These Se-NPs were characterized using UV-Visible spectroscopy (UV-Vis), Fourier transform (FT-IR) infrared spectroscopy and transmission (TEM) electron microscopy. The FT-IR spectrum confirms the presence of various functional groups in the aqueous tamarind fruit extract of, which may possibly influence the reduction process of the nanoparticles. TEM analysis determined that the size of the Se-NPs ranges from 2.34 to 49.86 nm. The nanoparticle suspension exhibited significant antimicrobial activity against *H. pylori* and able to inhibit the cell growth as revealed by SEM analysis.

Keywords: Antibacterial; Biosynthesis; *Tamarindus indica*; Mode of action; Nanomaterials.

1. Introduction

Nanotechnology is one of the most rapidly developing fields of science in the previous decade (Bayda *et al.*, 2019). This topic's research interest is growing, particularly in the field of nanoparticles (NPs) (particle sizes ranging from 1 to 100 nm) (Khan *et al.*, 2022). These NPs' uses have expanded to the treatment of different complex diseases as well as other domains such as biomedical and food industries (Mohammad *et al.*, 2022).

Nanotechnology evolved as the achievement of science in the 21st century. The synthesis, management, and application of those materials with a size smaller than 100 nm fall under the interdisciplinary umbrella of this field. Nanoparticles have significant applications in different sectors such as the environment, agriculture, food, biotechnology, biomedical, medicines, etc. like; for treatment of waste water, environment monitoring, as a functional food additives (Chen *et al.*, 2023), and as a antimicrobial agents (Islam *et al.*, 2022).

Bio-nanotechnology has an emerging important scientific role in the development of reliable eco-friendly techniques for the synthesis of nanoscale biomaterials using natural sources (Shah *et al.*, 2015)

There are several biomolecules or green plant extracts that have already been reported for the production of different kinds of nanomaterials such as metal nanoparticles, graphene (Sireesh Babu 2017; Sireesh Babu *et al.*, 2015, 2017a, b, 2018). This is because the production of nanoparticles via green synthesis has high compatibility, lower toxicity, environmental friendliness, and cost efficiency compared to the physical and chemical approaches (Pal *et al.*, 2018). The utilization of phyto-

based NP synthesis is of tremendous interest because it is a reasonably simple and quick procedure that does not require a reaction environment (Tavangar *et al.*, 2013).

Selenium (Se) is an essential trace element required by many organisms. It is a crucial cofactor of antioxidant enzymes such as glutathione peroxidases and thioredoxin reductases (Husen *et al.*, 2014 and Srivastava and Mukhopadhyay, 2013). As the selenium nanoparticles (SeNPs) possess antimicrobial and anticancer properties, they can be used as nanomedicines (Wadhvani *et al.*, 2016). Also, they exhibit less toxicity as compared to their inorganic and organic counterparts (Shakibaie *et al.*, 2010).

SeNPs can be produced by chemical, physical, or biological methods and their physicochemical characteristics depend on the methodology used (Ikram *et al.*, 2021).

In SeNPs biosynthesis process, reducing and stabilizing agents are the main factors. Biomolecules present in the extracts of plants, such as polysaccharides, phenolic compounds, flavonoids, tannins, saponins, amino acids, enzymes, proteins, and sugars, are known to be potential reducing agents of selenium and have medicinal importance. Some authors reported that the used plant extracts contained phytochemicals that exhibited stabilizing properties (Bartosiak *et al.*, 2019; Ingole *et al.*, 2010; Li *et al.*, 2010; Guleria *et al.*, 2020; Alagesan and Venugopal., 2019).

Biological synthesis of SeNPs is safe, eco-friendly, inexpensive and non-toxic (Wadhvani *et al.*, 2016). The use of plant extracts for the synthesis of nanoparticles might be beneficial over microbial synthesis by eliminating the extravagant procedures for maintaining cultures. Despite the fact, that a large number of plants are reported for nanoparticle synthesis, only few reports are available on phytochemical synthesis of SeNPs. These studies include synthesis using leaf extract of *Capsicum annum* (Li *et al.*, 2007), seed extract of fenugreek (Ramamurthy *et al.*, 2013), leaf extract of lemon (Prasad *et al.*, 2013), dried fruit extract of *Vitis vinifera* (Sharma *et al.*, 2014), leaf extract of *Terminalia arjuna* (Prasad and Selvaraj, 2014), flower extracts of *Bougainvillea spectabilis* (Deepa and Ganesan, 2014), leaf extract of *Leucas lavandulifolia* (Kirupagaran *et al.*, 2016), leaf extract of *Clausena dentate* (Sowndarya *et al.*, 2017), aqueous extract of *Allium sativum* (Anu *et al.*, 2017), leaf extracts of *Diospyros montana* (Kokila *et al.*, 2017), leaf extracts of *Psidium guajava* (Alam *et al.*, 2018), polysaccharides from *Lycium barbarum* and green tea extracts (Zhang *et al.*, 2018).

SeNPs have been synthesized by cell plant and fruit peel extracts as *Aloe vera* leaf extract (Fardsadegh and Jafarizadeh-Malmiri., 2019), *Eropegia bulbosa* Roxb extract (Cittrarasu *et al.*, 2021), *Azolla pinnata* (Rajagopal *et al.*, 2021), *Withania somnifera* leaf extract (Alagesan and Venugopal., 2019), *Diospyros montana* leaf extract (Kokila *et al.*, 2017), and citrus peel (Alvi *et al.*, 2021). Biosynthesis of SeNPs by different plant extracts such as: *Allium sativum* (Babu *et al.*, 2017), dried vitis vinifera (Raisin) extract (Sharma *et al.*, 2014), fenugreek seed extract (Ramamurthy *et al.*, 2013), flower of *Bougainvillea spectabilis* Willd (Deepa and Ganesan, 2014) have been previously reported.

The aim of this study was to use the tamarind fruit. aqueous extract in order to prepare SeNPs by an eco-friendly method. SeNPs were characterized by using various analytical techniques such as: SEM, UV-Vis spectroscopy and FTIR and to determine its antimicrobial activity against *H.pylori*.

2. Materials and Methods

2.1. Green Synthesis of *Tamarindus indica* fruit selenium nanoparticles

The extract was prepared by taking 2 g of *Tamarindus indica* fruit in 250 mL Erlenmeyer flask containing 50 ml of hot deionized water for 5 min. Then tamarind was squeezed well. The extract of *T. indica* fruit was filtered using Whatman 41 paper and was centrifuged at 7000 rpm for 15 min and stored at 4°C until using. A 50 mM sodium selenite solution was prepared by adding 86.47 mg sodium selenite powder to 10 mL of double-distilled water. Then 5 mL of the sodium selenite solution was added dropwise to 20 mL of an aqueous Tamarind fruit extract under magnetic stirring at room temperature. The mixture was incubated at room temperature. After 24 h of incubation, the mixture was centrifuged. 1 mL of this solution was used for UV-Vis analysis. The product was washed with dil. H₂O/ethanol and dried overnight. The formation of the Se-NPs was stored at 4–5 °C and submitted to additional testing

2.2. Characterization techniques

2.2.1. UV-visible analysis.

The UV-visible spectrum of the selenium nanoparticle solution was recorded using a double beam spectrophotometer (model T80+ UV-Vis spectrophotometer). The absorbance was measured in the range 200 to 800 nm. The absorbance peak was noted.

2.2.2. Fourier Transform Infrared (FTIR) Spectroscopy

A Fourier transform infrared spectrophotometer (Shimadzu IRAffinity-1, Kyoto, Japan) was used in order to determine the responsible phytochemical compounds with various functional groups that act as the reducing and capping agents in the aqueous Tamarind fruit extract and to study their potential role in the fabrication of T-SeNPs. The T-SeNPs solution was characterized by scanning the spectra in the range of 4000–400 cm^{-1} wavenumbers in KBr pellets.

2.2.3. Transmission (TEM) Electron Microscopy

The transmission electron microscopy (JEOL JEM-F200, Tokyo, Japan) was executed to determine the size distribution and the exact shape of the T-SeNPs. The T-SeNPs were sonicated and set carefully on a copper coated grid to be viewed under the microscope.

2.2.4. *Helicobacter pylori* strains

Two strains of *H. pylori* strains (i.e ATCC- 700392 and clinical isolate registered in gene bank with ID: OK298394.1) were employed in current study. The bacteria were routinely propagated in ATCC Medium 260 “Trypticase soy agar/broth with defibrinated sheep blood” under microaerophilic conditions (e.g. 10% CO_2 , 85% N_2 and 5% O_2) at 37 °C.

2.2.5. Antimicrobial activity of Se NPs against *H.pylori*

The selenium nanoparticles synthesized from Tamarind extract were tested for their antimicrobial activity by well diffusion method against pathogenic organism. The diffusion in agar test was carried out in line with the Clinical Laboratory Standard Institute's guideline M51-A2 (Standard NCfCL) with minor modifications. At 37 °C, the selected bacterial strain was grown for 24 h on Brain heart broth medium. Bacterial suspension of 1.5×10^6 CFU mL^{-1} was separately prepared, seeded into Columbia blood agar medium, and poured aseptically into sterilized plates. A 100 μL of 0.01, 0.1 and 1.0 % concentration (w/v) of T-SeNPs, compared to standard antibiotic (Trio-clar, Sigma Aldrich; 0.1 % concentration) were pipetted into 6 mm wells in inoculated plates, then plates were put in refrigerator for 2 h followed by incubation at 37°C for 24 h in a microaerobic atmosphere (10% CO_2 , 85% N_2 and 5% O_2) then the inhibition-zone diameter was measured.

2.2.6. Scanning (SEM) electron microscopy imaging of treated bacteria

Bacterial cells (*H. pylori* OK298394.1) at $\text{OD}_{600} = 0.2$ were mixed with T-SeNPs (1 mg/mL) and incubated at 37 °C for 5 h under shaking (agitation 150 rpm). Scanning (SEM) electron microscopy (JEOL JSM-7600F, Tokyo, Japan) imaging was performed to identify the surface morphology alteration of treated bacteria. Bacterial cells were collected by centrifugation and dehydrated with serial ethanol concentrations, then coated with gold/pladium using a sputter coater before the samples were filled into their holders.

3. Results

Green Synthesis of *Tamarindus indica* fruit selenium nanoparticles

Visual observation

Reduction of metal salts into metal nanoparticles by the bio-molecules is always accompanied by the colour change of reaction medium. In the present study the colourless solution of sodium selenite is changed in brick red colour after addition of Tamarind extract at 24 hour as shown in Figure 1(A).

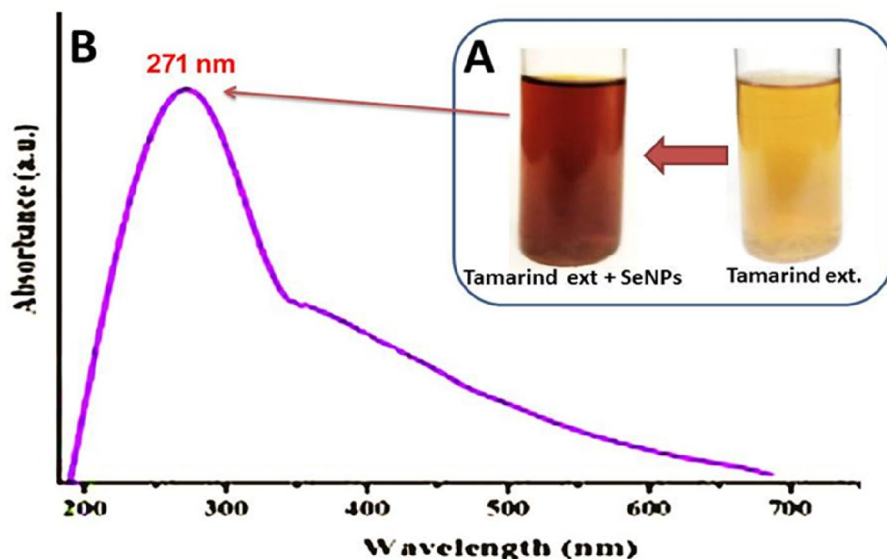


Fig. 1: Color indicators of the mixture of tamarind aqueous fruit extract and selenite solution indicating their visual color change after interaction (A) and their UV-vis spectra after SeNPs synthesis (B), for 24 h.

Characterization techniques using UV analysis

The biosynthesized T-SeNPs were primarily characterized by UV-visible analysis. In general, wavelengths of light in the range of 200–800 nm are usually used for characterizing various metal nanoparticles. Therefore, the T-SeNPs were characterized by measuring the absorbance in the wavelength range from 200 to 800 nm. Figure 1(B) exhibits the UV-vis spectrum of synthesized SeNPs with maximum absorption at 271 nm.

FTIR Analysis

FTIR was used to analyze the characteristics of the biomolecules that are involved in the reduction, capping, and stability of selenium metal. As seen in Figure 2, the FTIR spectra of the tamarind extract revealed a number of functional groups. Some notable characteristic peaks were seen at 3407 cm^{-1} , 2931 cm^{-1} , 1633 cm^{-1} , 1408 cm^{-1} , and 1071 cm^{-1} . The tamarind extract produced selenium nanoparticles show peaks at 3358 cm^{-1} , 2923 cm^{-1} , 1742 cm^{-1} , 1415 cm^{-1} , and 1069 cm^{-1} .

The extract's spectra showed an intense, sharp peak centered at 3407 cm^{-1} , which was attributed to the stretching vibration of the N-H group. Additionally, a solitary peak of C=O of carbonyl group emerged at 1633 cm^{-1} , adjacent to a minuscule peak at 1071 cm^{-1} caused by the stretching vibrations of -C=O (ester). These peaks confirmed the existence of Tamarind extract's active ingredients, which include heterocyclic chemicals (alkaloids, flavonoids, and alkaloids) that serve as SeNPs' capping agent. However, as Figure 2 illustrates, notable modifications were seen following the incorporation of selenium nanoparticles. Compared to the FT-IR spectra of pure Tamarind extract, the band locations of Tamarind extract capped SeNPs at 3358 cm^{-1} , 2923 cm^{-1} , 1069 cm^{-1} , and 1042 cm^{-1} are slightly moved to lower wave number. The shift indicated that the creation of SeNPs reduces the strength of -OH vibration, as evidenced by the broadening of the peaks at 3358 and 2923 cm^{-1} . Following the synthesis of SeNPs, a new peak emerged in 1742 , while the intensity of the peak that first emerged at 1633 dropped. The metal-ligand stretching frequency that may arise from biomolecules interacting with the surfaces of selenium nanoparticles is what causes the peaks at 500 cm^{-1} .

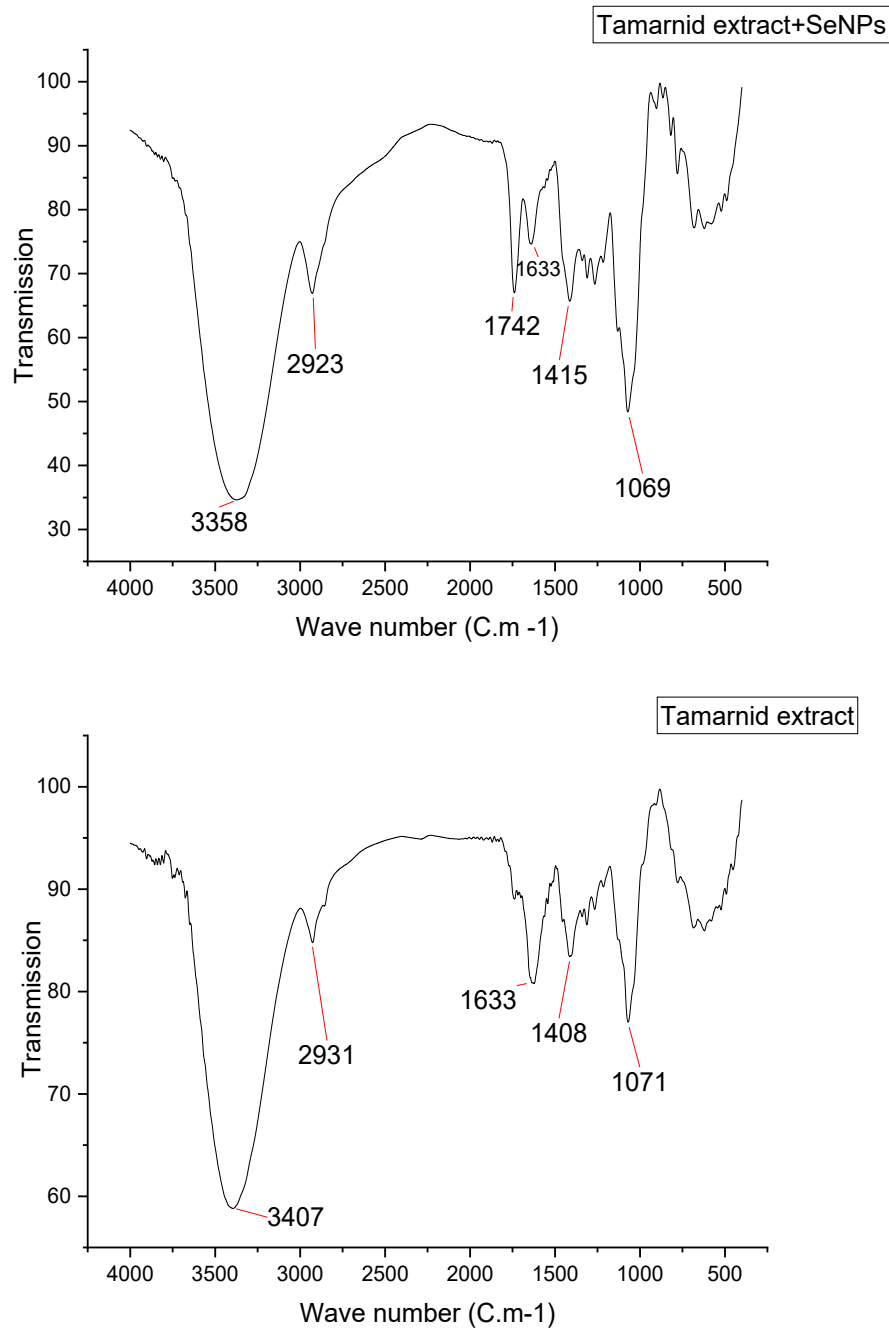


Fig. 2: FTIR spectra of *Tamrind* fruit extract and T-SeNPs.

Transmission Electron Microscopy (TEM)

To verify the size and morphology of the synthesized T-SeNPs, TEM analyses of sample Se (e) were also performed. The high magnification of the TEM image in Figure 3 shows that the T-SeNPs have an almost spherical shape with different sizes. The TEM image also shows that the T-SeNPs are well distributed in powder form with slight agglomeration. Figure 3 shows that the diameter of the T-SeNPs is in the range of 2.34–49.86 nm.

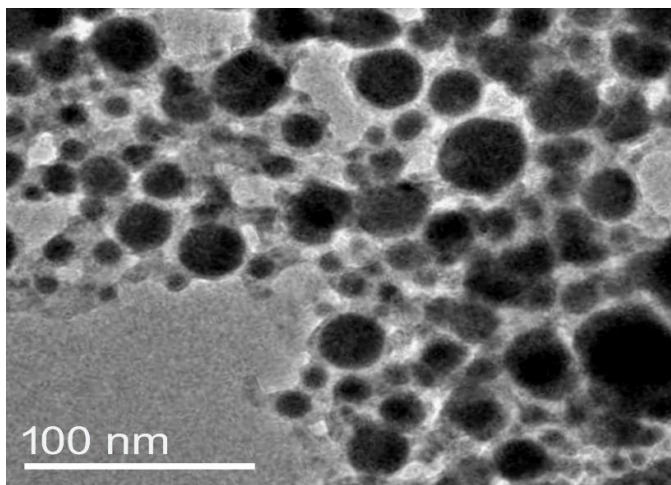


Fig. 3: TEM imaging of T-SeNPs

Antimicrobial activity of SeNPs against *H. pylori*

Results illustrated that T-SeNPs exhibited promising antibacterial activity against *H.pylori* as compared with the control. The antibacterial activity of T-SeNPs toward *H. pylori* strains are appointed in Table 1.

Table 1: Antimicrobial activity of tamarind-synthesized SeNPs against *Helicobacter pylori* strains

Antibacterial agent (concentration)	Inhibition zone (mm)*	
	<i>H. pylori</i> ATCC- 700392	<i>H. pylori</i> OK298394.1
T-SeNPs (0.01 %)	10.6 ± 0.8	10.9 ± 1.1
T-SeNPs (0.1 %)	15.3 ± 1.1	16.5 ± 1.5
T-SeNPs (1.0 %)	23.2 ± 2.4	25.1 ± 2.8
Trio-clar (0.1 %)	16.7 ± 1.3	17.2 ± 1.6

* Diameter are triplicates’ mean included 6 mm (wells diameter) ± SD

The T-SeNPs based solutions exhibited notable anti- *H. pylori* activity, which was correlated with the nanomaterials concentrations. At the same concentration (i.e. 0.1 %, w/v), the activity of T-SeNPs was comparable to the standard antibiotic Trio-clar, toward the two challenged *H. pylori* strains. The strain *H. pylori* OK298394.1 was generally more susceptible than the standard strain (*H. pylori* ATCC- 700392) to the nanomaterial and the antibiotic.

Scanning (SEM) microscopy imaging of exposed bacteria

SEM imaging was applied in order to show changes at bacterial structure upon their interactions with SeNPs. In medium free of SeNPs, *H. pylori* was normal in Fig. 4(C). The untreated bacterial cells were in rod shapes with intact cell structure. SEM images show that *H. pylori* treated with T- SeNPs to the medium-induced morphological changes of bacteria cells at the membrane level (Fig. 4-T). Those changes reflect the formation of irregular cell surface and alteration of cell membrane. Curiously, when T-SeNPs were added to the bacterial solution, almost no integral cell was observed suggesting the leakage of the internal cell content. Also, SEM analysis showed that T-SeNPs cause extensive injury of the bacterial cell membrane and complex morphological changes. Moreover, some cellular debris associated with the nanoparticles was also detected.

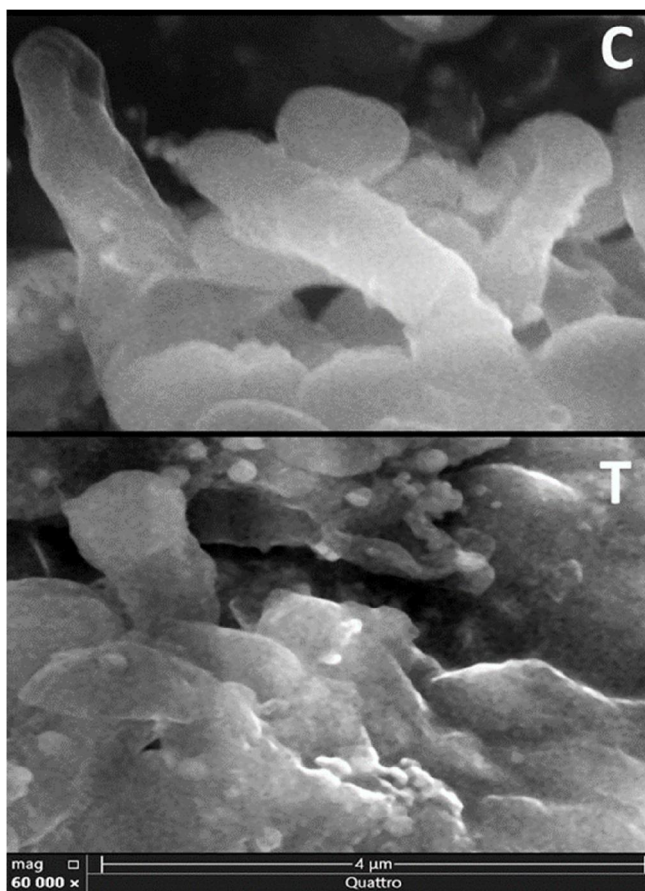


Fig. 4: (c) SEM imaging of control *H. pylori* cells and (T) SEM imaging of *H. pylori* treated with T-SeNPs.

4. Discussion

The synthesized or fabricated Se nanoparticles were identified visually by time-dependent color variation during mixture reaction. The solution changes color from pale yellow to brick red. After the incubation time of 24 hours, no further color variation was observed similar result was obtained by Rashna *et al.* (2023). The morphology characteristics of the nanoparticle is achieved by SEM which is of great impact as morphology always influences most of the nanoparticle properties. Characterization of structure is significant to study the nature and composition of bond materials. UV-visible spectroscopy is used for the optical features of T-selenium nanoparticles. The biosynthesized Se nanoparticles has spherical structures with particle diameter range of in the range of 2.34–49.86 nm. similar result was obtained by Rashna *et al.* (2023) he found that the structure morphology of synthesized Se nanoparticles having average particle size of 50 nm. Another results obtained by some author like (Shakibaie *et al.*, 2015) also formed spherical Se nanoparticles having huge frequency of 120-140 nm within the range of 80-220 nm. Similar results of SEM at 200 nm were found in (Salem *et al.*, 2022).

The results of UV visible spectra of T- Se nanoparticles shows absorbance peaks at wavelength of 271 nm The obtained results of Se nanoparticles are in accordance with absorbance data in literature (Alagesan & Venugopal, 2019). This can be concluded from the absorbance spectra that biosynthesized nanoparticles are visible active and can be applied in various fields due to their characteristic sensor properties.

The FTIR spectra of the tamarind extract revealed a number of functional groups. Some notable characteristic peaks were seen at 3407 cm^{-1} , 2931 cm^{-1} , 1633 cm^{-1} , 1408 cm^{-1} , and 1071 cm^{-1} . The tamarind extract produced selenium nanoparticles show peaks at 3358 cm^{-1} , 2923 cm^{-1} , 1742 cm^{-1} , 1415 cm^{-1} , and 1069 cm^{-1} .

The extract's spectra showed an intense, sharp peak centered at 3407 cm^{-1} , which was attributed to the stretching vibration of the N-H group. Additionally, a solitary peak of C=O of carbonyl group emerged at 1633 cm^{-1} , adjacent to a minuscule peak at 1071 cm^{-1} caused by the stretching vibrations of -C=O (ester). These peaks confirmed the existence of Tamarind extract's active ingredients, which include heterocyclic chemicals (alkaloids, flavonoids, and alkaloids) that serve as SeNPs' capping agent. However, as Figure 2 illustrates, notable modifications were seen following the incorporation of selenium nanoparticles. Compared to the FT-IR spectra of pure Tamarind extract, the band locations of Tamarind extract capped SeNPs at 3358 cm^{-1} , 2923 cm^{-1} , 1069 cm^{-1} , and 1042 cm^{-1} are slightly moved to lower wave number. The shift indicated that the creation of SeNPs reduces the strength of -OH vibration, as evidenced by the broadening of the peaks at 3358 and 2923 cm^{-1} . Following the synthesis of SeNPs, a new peak emerged in 1742 , while the intensity of the peak that first emerged at 1633 dropped. The metal-ligand stretching frequency that may arise from biomolecules interacting with the surfaces of selenium nanoparticles is what causes the peaks at 500 cm^{-1} . The transition of selenium metal ions into selenium nanoparticles may be due to the phytochemicals present in the extract, as previously mentioned. This finding is supported by Jayaprakash *et al.* (2017)

Previous reports have also suggested the role of phytochemicals as a stabilizing agent for the synthesis of metal NPs (Coccia *et al.*, 2012).

Phenolic compounds, flavonoids and minerals present in plant materials may facilitate the synthesis of nanoparticles (Sharma *et al.*, 2014). From the phenols class, flavonoids are predominant compounds in parsley. In the aqueous extract of parsley leaves, apigenin (4', 5, 7-trihydroxyflavone), cosmosiin (apigenin-7-O-glucoside), oxypeucedanin hydrate (coumarin 2",3"-dihydroxyfuranocoumarin) and apiin (apigenin-7-O-apiosyl-(1 --> 2)-O-glucoside) were detected.

Nanomaterials as antibacterials complementary to antibiotics are highly promising and are gaining large interest as they might fill the gaps where antibiotics frequently fail. This includes combatting multidrug-resistant mutants and biofilm (Pelgrift and Friedman, 2013; Zhang *et al.*, 2018). *In vitro* and *in vivo* studies have shown that antibacterial nanoparticles can suppress infection (Qu *et al.*, 2013 and Hashem *et al.*, 2022). Furthermore, antimicrobial nanoparticles may harm bacteria in a variety of ways, making it harder for bacteria to acquire resistance (Huh and Kwon, 2011).

The mechanism of action of metal nanoparticles as antimicrobial agents is attributed to different mechanisms: (1) metabolic interference via intercellular adenosine triphosphate (ATP) concentrations, (2) intracellular reactive oxygen species (ROS) concentration modulation, (3) bacterial membrane depolarization, and (4) bacterial membrane interruption. ATP is an internal energy that is used by all living organisms. It is an important source of energy for respiration and metabolism (Mempin, *et al.*, 2013). Virulence factors of bacteria, such as sluggish drug absorption and rapid efflux, biofilm development, and intracellular bacterial parasitism, have been proven to be overcome by these nanoparticles (Pelgrift and Friedman 2013).

The rapid spread of antibiotic-resistant *Mtb* strains makes it necessary to search for alternative treatments. In this sense, the use of nanoparticles with mycobactericidal potential could be especially interesting, since nanoparticles have a high surface area, which means that they contain a high number of active sites to be able to interact with biological entities and, on the other hand, they have a high capacity to penetrate cells and tissues (Lu *et al.*, 2018; Singh *et al.*, 2015). SeNPs have been shown to have antimicrobial activity against different types of bacteria (Huang *et al.*, 2019).

The limited mechanism has been reported by few references in the antibacterial property of bio-SeNPs. Beheshti *et al.*, (2013) reported that bio-SeNPs synthesized by *Bacillus* sp. could induce apoptosis of protozoa *Leishmania major* through DNA fragmentation. Besides, observed that the addition of bio-SeNPs could effectively promote the production of reactive oxygen species (ROS), but their intensity did not show size- or shape-dependent effect. And other unknown mechanisms still need to be discovered. However, the antimicrobial activity of other nanoparticles was generally achieved by the damage of mitochondria, disruption of cell membranes and even interrupting the transmembrane electron transport.

Henglin *et al.*, 2021 they synthesized spherical bio-SeNPs with an average size of 120 nm were synthesized by strain *Providencia* sp. DCX. The SeNPs were further applied to investigate the antibacterial properties of model bacteria, including Gram-positive (*Staphylococcus aureus*, *Bacillus cereus* and *Bacillus subtilis*) and Gram-negative bacteria (*Pseudomonas aeruginosa*, *E. coli* and *Vibrio parahaemolyticus*). The biosynthesized SeNPs demonstrated strong inhibition activity against the growth

of these pathogens. When treated with 500 mg/L SeNPs, most of the tested bacteria were destructed within 12 h, among which the mortality rates of Gram-negative bacteria were much better. The leakage tests illustrated that there existed more proteins and polysaccharides outside the cells after reacted with bio-SeNPs. It was indicated that the leakages of proteins and polysaccharides were caused by permeability changes of membranes and the disruption of cell walls. And the change of reactive oxygen species (ROS) intensity indicated that oxidative damage may play the significant role in the antibacterial processes.

5. Conclusion

Nano-particles can be produced in a cost-effective manner with no toxic by-products using green synthesis. The biological technique based on plant extract is the most popular form of green synthesis. In conclusion, this study has shown that T-SeNPs can be synthesized using the plant extract of *Tamarindus indica*. The extract of polyphenol components and the water soluble heterocyclic components such as alkaloid and flavones were principally responsible for the reduction of selenium ions and the stabilization of the nanoparticles. FT-IR spectra revealed the presence of reducing groups in extract for Se NPs synthesis. The synthesized selenium nanoparticles shows spherical shape with average diameter range is 2.34–49.86 nm.

Green synthesized selenium nanoparticles could be a potential antibacterial agent to treat diseases caused by *H. pylori*.

References

- Alvi, G.B., M.S. Iqbal, M.M.S. Ghaith, A. Haseeb, B. Ahmed, and M.I. Qadir, 2021. Biogenic Selenium Nanoparticles (SeNPs) from Citrus Fruit Have Anti-Bacterial Activities. *Sci. Rep.*, 11, 4811.
- Alagesan, V., and S. Venugopal, 2019. Green Synthesis of Selenium Nanoparticle Using Leaves Extract of *withania somnifera* and Its Biological Applications and Photocatalytic Activities. *Bionanoscience*, 9: 105–116.
- Alam, H., N. Khatoon, M. Raza, P.C. Ghosh, and M. Sardar, 2018. Synthesis and characterization of nano selenium using plant biomolecules and their potential applications. *BioNanoScience*, 9: 96–104.
- Anu, K., G. Singaravelu, K. Murugan, and G. Benelli, 2017. Green-synthesis of selenium nanoparticles using garlic cloves (*Allium sativum*): biophysical characterization and cytotoxicity on vero cells. *J. Cluster Sci.* 28: 551–563.
- Beheshti, N., S. Soflaei, M. Shakibaie, M.H. Yazdi, F. Ghaffarifar, A. Dalimi, and A.R. Shahverdi, 2013. Efficacy of biogenic selenium nanoparticles against *Leishmania major*: in vitro and in vivo studies. *Journal of Trace Elements in Medicine and Biology*, 27(3): 203-207.
- Bartosiak, M., J. Giersz, and K. Jankowski, 2019. Analytical monitoring of selenium nanoparticles green synthesis using photochemical vapor generation coupled with MIP-OES and UV-Vis spectrophotometry. *Microchem. J.* 145: 1169–1175.
- Bayda S., M. Adeel, T. Tuccinardi, M. Cordani, and F. Rizzolio, 2019. The history of nanoscience and nanotechnology: from chemical–physical applications to nanomedicine. *Molecules* 25:112. 10.3390/molecules25010112
- Chen J., Y. Guo, X. Zhang, J. Liu, P. Gong, Z. Su, *et al.*, 2023. Emerging nanoparticles in food: sources, application, and safety. *J. Agricult. Food Chem.* 71: 3564–3582.
- Cittrarasu, V., D. Kaliannan, K. Dharman, V. Maluventhen, M. Easwaran, W.C. Liu, B. Balasubramanian, and M. Arumugam, 2021. Green Synthesis of Selenium Nanoparticles Mediated from *Ceropegia bulbosa* Roxb Extract and Its Cytotoxicity, Antimicrobial, Mosquitocidal and Photocatalytic Activities. *Sci. Rep.*, 11: 1032.
- Coccia, F., L. Tonucci, D. Bosco, M. Bressand, and N. d’Alessandro, 2012. One pot synthesis of lignin-stabilized platinum and palladium nanoparticles and their catalytic behavior on oxidation and reduction reactions. *Green Chemistry*, 14: 1073–10.
- Deepa, B., and V. Ganesan, 2014. Bioinspired synthesis of selenium nanoparticles using flowers of *Catharanthus roseus* (L.) G. Don. and *Peltophorumpterocarpum* (DC.) backer ex Heyne—a comparison. *Int. J. Chem. Tech. Res.* 2015:2.

- Fardsadegh, B., and H. Jafarizadeh-Malmiri, 2019. Aloe Vera Leaf Extract Mediated Green Synthesis of Selenium Nanoparticles and Assessment of Them *in vitro* Antimicrobial Activity against Spoilage Fungi and Pathogenic Bacteria Strains. *Green Process. Synth.*, 8: 399–407.
- Guleria, A., S. Neogy, B.S. Raorane, and S. Adhikari, 2020. Room temperature ionic liquid assisted rapid synthesis of amorphous Se nanoparticles: their prolonged stabilization and antioxidant studies. *Mater. Chem. Phys.* 253: 123369.
- Henglin Z., L. Zhang, D. Chunxiao, W. Pin, F. Shuling, Y. Bib, and Q. Yuanyuan, 2021. Antibacterial properties and mechanism of selenium nanoparticles synthesized by *Providencia* sp. DCX. *Environmental Research.* 149: 110630.
- Huh, A.J., and Y.J. Kwon, 2011. “Nanoantibiotics”: A new paradigm for treating infectious diseases using nanomaterials in the antibiotics resistant era. *J. Control. Release Off. J. Control. Release Soc.*, 156: 128–145.
- Husen, A., and K.S. Siddiqi, 2014. Plants and microbes assisted selenium nanoparticles: characterization and application. *J. Nanobiotechnol.*, 12:28.
- Huang, T., J.A. Holden, D.E. Heath, N.M. O’Brien-Simpson, and A.J. O’Connor, 2019. Engineering highly effective antimicrobial selenium nanoparticles through control of particle size. *Nanoscale*, 11: 14937–14951. doi: 10.1039/c9nr04424h.
- Hashem, A.H., A.M. Shehabeldine, O.M. Ali, and S.S. Salem, 2022. Synthesis of Chitosan-Based Gold Nanoparticles: Antimicrobial and Wound-Healing Activities. *Polymers*, 14, 2293.
- Ikram M., B. Javed, N.I. Raja, and Z.-U.-R. Mashwani, 2021. Biomedical potential of plant-based selenium nanoparticles: a comprehensive review on therapeutic and mechanistic aspects *Int. J. Nanomed.*, 16: 249-268.
- Ingole, A.R., S.R. Thakare, N.T. Khati, A.V. Wankhade, and D.K. Burghate, 2010. Green synthesis of selenium nanoparticles under ambient condition. *Chalcogenide Lett.* 7: 485–489.
- Islam F., S. Shohag, M.J. Uddin, M.R. Islam, M.H. Nafady, A. Akter, et al. (2022). Exploring the journey of zinc oxide nanoparticles (ZnO-NPs) toward biomedical applications. *Materials* 15:2160.
- Jayaprakash, N., J. Vijayaj, K. Kaviyarasu, K. Kombaiyah, L.J.R. Kennedy R.J. Jothi Ramalingam, A. Murugan M.A. Munusamy, and H.A. Al-Lohedan, 2017. Green synthesis of Ag nanoparticles using Tamarind fruit extract for the antibacterial studies *J. PhotochemPhotobiol B.* 169:178-185.
- Khan, A.M., H. Yasmin, A.Z. Shah, J. Rinklebe, Mohammed Nasser Alyemeni N. M., and P. Ahmad, 2022. Co application of biofertilizer and zinc oxide nanoparticles upregulate protective mechanism culminating improved arsenic resistance in maize. *Chemosphere*, 294:133796.
- Kirupagaran, R., A. Saritha and S. Bhuvaneshwari, 2016. Green Synthesis of Selenium Nanoparticles from Leaf and Stem Extract of *Leucas lavandulifolia* Sm. and Their Application. *Journal of Nanoscience and Technology* 2(5): 224–22.
- Kokila, K., N. Elavarasan, and V. Sujatha, 2017. *Diospyros montana* leaf extract-mediated synthesis of selenium nanoparticles and their biological applications. *New J. Chem.* 41: 7481–7490.
- Li, S., Y. Shen, A. Xie, X. Yu, X. Zhang, L. Yang, and C. Li, 2007. Rapid, room-temperature synthesis of amorphous selenium/protein composites using *Capsicum annuum* L extract. *Nanotechnology.* Sep 11;18(40):405101.
- Lu, T., Y. Wu, C. Zhao, F. Su, J. Liu, Z. Ma, et al., 2018. One-step fabrication and characterization of Fe₃O₄/HBPE-DDSA/INH nanoparticles with controlled drug release for treatment of tuberculosis. *Mater. Sci. Eng. C Mater. Biol. Appl.* 93: 838–845.
- Mempin, R., H. Tran, C. Chen, H. Gong, K. Kim Ho, and S. Lu, 2013. Release of extracellular ATP by bacteria during growth. *BMC Microbiol.*, 13, 301.
- Mohammad, Z.H., F. Ahmad, S.A. Ibrahim, and S. Zaidi, 2022. Application of nanotechnology in different aspects of the food industry. *Discover Food*, 2(1):12.
- Pelgrift, R.Y., and A.J. Friedman, 2013. Nanotechnology as a therapeutic tool to combat microbial resistance. *Adv. Drug Deliv. Rev.*, 65: 1803–1815.
- Prasad, K.S., H. Patel, T. Patel, K. Patel, and K. Selvaraj, 2013. Biosynthesis of Se nanoparticles and its effect on UV-induced DNA damage. *Colloids Sur. B Biointerfaces*, 103: 261–266.

- Prasad, K.S., and K. Selvaraj, 2014. Biogenic synthesis of selenium nanoparticles and their effect on as (III)-induced toxicity on human lymphocytes. *Biol. Trace Elem. Res.* 157: 275–283. doi: 10.1007/s12011-014-9891-0
- Pal, G., P. Rai, and A. Pandey, 2018. *Green Synthesis of Nanoparticles: A Greener Approach for a Cleaner Future*; Elsevier Inc.: Amsterdam, The Netherlands, ISBN 9780081025796
- Qu, X., J. Brame, Q. Li, and P.J.J. Alvarez, Nanotechnology for a Safe and Sustainable Water Supply: Enabling Integrated Water Treatment and Reuse. *Acc. Chem. Res.* 46: 834–843.
- Rajagopal, G., A. Nivetha, S. Ilango, G.P. Muthudevi, I. Prabha, and R. Arthimanju, 2021. Phytofabrication of selenium nanoparticles using *Azolla pinnata*: Evaluation of catalytic properties in oxidation, antioxidant and antimicrobial activities. *Journal of Environmental Chemical Engineering*, 9(4): 105483.
- Ramamurthy, C.H., K.S. Sampath, P. Arunkumar, M.S. Kumar, V. Sujatha, K. Premkumar, *et al.*, 2013. Green synthesis and characterization of selenium nanoparticles and its augmented cytotoxicity with doxorubicin on cancer cells. *Bioprocess Biosyst. Eng.* 36: 1131–1139.
- Rashna A., A. Samreen, L. Atif, S. Muhammad, J.C. Muhammad Farhan, N. Muhmmad, A.F. Muhammad, M. Tariq, and K. Adnan, 2022. Green-synthesized selenium nanoparticles using garlic extract and their application for rapid detection of salicylic acid in milk. *Food Sci. Technol, Campinas*, 43, e67022, 2023
- Shah, M., D. Fawcett, S. Sharma, S.K. Tripathy, and G.E.J. Poinern, 2015. Green Synthesis of Metallic Nanoparticles via Biological Entities. *Materials*, 8:7278-7308.
- Shakibaie, M., M. Khorramizadeh, M. Faramarzi, O. Sabzevari, and A. Shahverdi, 2010. Biosynthesis and recovery of selenium nanoparticles and the effects on matrix metalloproteinase-2 expression. *Biotechnol Appl Biochem.*, 56(1):7–15
- Shakibaie, M., H. Forootanfar, Y. Golkari, T. Mohammadi-Khorsand, and M.R. Shakibaie, 2015. Antibiofilm activity of biogenic selenium nanoparticles and selenium dioxide against clinical isolates of *Staphylococcus aureus*, *Pseudomonas aeruginosa*, and *Proteus mirabilis*. *Journal of Trace Elements in Medicine and Biology*, 29: 235-241.
- Sharma, G., A.R. Sharma, R. Bhavesh, J. Park, B. Ganbold, J.S. Nam, and S.S. Lee, 2014. Biomolecule-mediated synthesis of selenium nanoparticles using dried *Vitis vinifera* (raisin) extract. *Molecules* 19: 2761–2770.
- Singh, R., L.U. Nawale, M. Arkile, U.U. Shedbalkar, S.A. Wadhvani, D. Sarkar, *et al.*, 2015. Chemical and biological metal nanoparticles as antimycobacterial agents: a comparative study. *Int. J. Antimicrob. Agents*, 46: 183–188. doi: 10.1016/j.ijantimicag.2015.03.014.
- Sireesh Babu, M., M. Badal Kumar, and A. Kiran Kumar, 2017a. Environment friendly approach for size controllable synthesis of biocompatible silver nanoparticles using diastase. *Environ Toxicol Pharmacol.*, 49:131–136.
- Sireesh, B.M., K.M. Badal, and K.A. Kiran, 2017b. Tyrosine assisted size controlled synthesis of silver nanoparticles and their catalytic and *in vitro* cytotoxicity evaluation. *Environ Toxicol Pharmacol.*, 51:23–29.
- Sireesh, B.M., K.M. Badal, R. Shivendu, and D. Nandita, 2015. Diastase assisted green synthesis of size controllable gold nanoparticles. *RSC Adv.*, 5:26727–26733
- Sireesh, B.M., S. Jegatheeswaran, S.Y. Serap, H. Guobin, C. Yurong, G. Junkuo, N. Qingqing, and J. Yao, 2018. Silk sericin induced fabrication of reduced graphene oxide and its *in vitro* cytotoxicity, photothermal evaluation. *J Photochem Photobiol B.*, 186:189–196.
- Sireesh, B.M., 2017. Green synthesis of biocompatible Au–Cu₂–xSe heterodimer nanoparticles and their *in vitro* photothermal assay. *Environ Toxicol Pharmacol.*, 53:29–33.
- Srivastava, N., and M. Mausumi, 2013. "Biosynthesis and structural characterization of selenium nanoparticles mediated by *Zooglea ramigera*." *Powder Technology*, 244: 26-29.
- Standard, NCFCL., 2002. *Reference method for broth dilution antifungal susceptibility testing of yeasts*. National Committee for Clinical Laboratory Standards Wayne
- Salem, S.S., M.S.E. Badawy, A.A. Al-Askar, A.A. Arishi, F.M. Elkady, and A.H. Hashem, 2022. Green biosynthesis of selenium nanoparticles using orange peel waste: charecterization, antibacterial and antibiofilm activities against multidrug-resistant bacteria. *Life (Basel, Switzerland)*, 12(6): 893. <http://dx.doi.org/10.3390/life12060893>. PMID:35743924.

- Sowndarya, P., G. Ramkumar, and M.S. Shivakumar, 2017. Green synthesis of selenium nanoparticles conjugated *Clausena dentata* plant leaf extract and their insecticidal potential against mosquito vectors. *Artif. Cells Nanomed. Biotechnol.*, 45: 1490–1495.
- Tavangar, A., B. Tan, and K. Veenkatakrishnan, 2013. Sustainable approach toward synthesis of green functional carbonaceous 3-D micro/nanostructures from biomass. *Nanoscale Research Letters*, 8(1):348.
- Wadhvani, S.A., U.U. Shedbalkar, R. Singh, and B.A. Chopade, 2016. Biogenic selenium nanoparticles: current status and future prospects. *Applied microbiology and biotechnology*, 100:2555-66.
- Zhang, W., J. Zhang, D. Ding, L. Zhang, L.A. Muehlmann, S.E. Deng, *et al.*, 2018. Synthesis and antioxidant properties of *Lycium barbarum* polysaccharides capped selenium nanoparticles using tea extract. *Artif. Cells Nanomed. Biotechnol.* 46: 1463–1470.
10.1080/21691401.2017.1373657